Paper 106

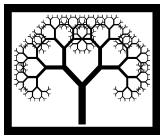

Proceedings of the Eleventh International Conference
on Computational Structures Technology,
B.H.V. Topping, (Editor),
Civil-Comp Press, Stirlingshire, Scotland

Fatigue Assessment of a Bowstring Railway Bridge

C. Albuquerque, R. Calçada and P.M.S.T. de Castro
Faculty of Engineering
University of Porto, Portugal

Abstract

The fatigue analysis of steel and composite bridges under real traffic is a challenging task. In situ monitoring of all the details of the structure is not economically (and even technically) feasible and consequently, numerical models are usually employed for that analysis. The common assumption is that if the numerical model reproduces well the real behaviour of the structure in some reference points, extrapolation of the numerical model results to other points is reasonable and accurate, from an engineering point of view. This paper, explores the different aspects of the fatigue analysis of the new Alcácer do Sal bridge, in Portugal, in the context of the FADLESS European project.

Keywords: fatigue, bridge, ambient vibration test, long term monitoring, dynamic analysis, FADLESS.

1 Introduction

The fatigue analysis of steel and composite bridges under real traffic is usually performed using numerical models of the structures, since in situ monitoring of all the details of each structure is not feasible. Nevertheless, for a numerical model to accurately reproduce the real response of a bridge, it must be calibrated and updated based on experimental data, gathered in in situ experimental campaigns.

This paper goes through the above mentioned aspects of the fatigue analysis of the new Alcácer do Sal bridge, in Portugal, in the context of the FADLESS European project. In section 2 a description of the bridge is performed, while in section 3 the numerical model of the bridge is presented. Section 4 focuses on the experimental work developed with the aim of characterize the structure. Finally, section 5 presents some of the results of the fatigue analysis performed on the structure, according to the Eurocode 3 [1].

2 The new Alcácer do Sal railway bridge

The new Alcácer do Sal railway bridge is located in the Lisboa – Algarve connection, in Portugal (Figure 1).

a) Location [2]

b) Overview [3]

Figure 1: New Alcácer do Sal Railway bridge

It is prepared for passenger trains (as the Alfa Pendular tilting train and the Intercity train) running at speeds up to 250 km/h. Since it is also part of the main railway connection to the sea port of Sines, it must be prepared for freight trains with up to 25 tons per axle (Figure 2).

a) Alfa Pendular train

b) Intercity train

c) Freight train

Figure 2: Typical traffic

The bridge has a continuous composite deck that covers three spans (160m per span). The deck is suspended from 3 arches. Each arch holds one span of the deck, with 18 vertical hangers, 8 m apart from each other (Figure 3). The structure is preceded by the north and south access viaducts (with 1115 m and 1140 m, respectively). Both viaducts and bridge are prepared to hold two ballasted tracks even if only the upstream track is on operation, at the current time.

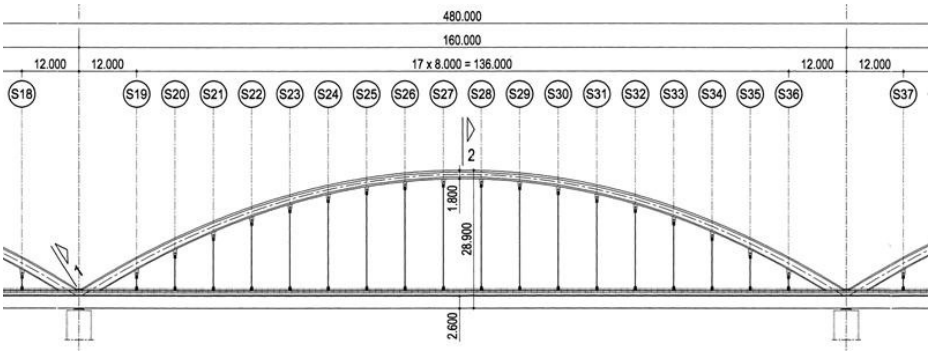

Figure 3: Side view of the midspan of the bridge [4]

A reinforced concrete slab above a U-shaped steel box forms the deck (Figure 4a). The 15.85 wide concrete slab has a maximum thickness of 0.43 m. The steel box, with sloped webs, was built up by welding steel plates. Maximum plate's thickness is 120 mm. A diaphragm reinforces the deck at each deck to hanger connection. Two diagonals per hanger distribute the suspension force to the deck. The arches present an hexagonal hollow section with variable height and width (Figure 4b) and Figure 4c)). In this case thick steel plates were also used and assembled by welding.

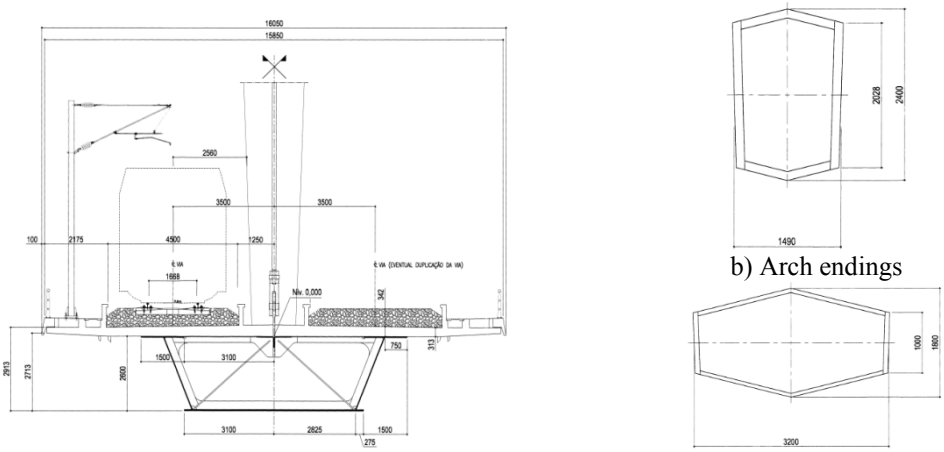

b) Arch endings

a) Deck

c) Arch's mid section

Figure 4: Typical cross sections of the bridge [4]

3 The numerical model

The global model of the bridge was developed with the software ANSYS, using shell, beam and mass elements (Figure 5).

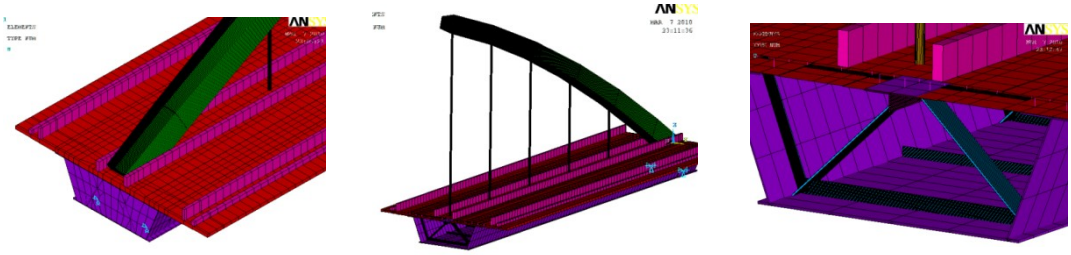

a) Deck and arch's ending

b) Cross section before 5th diaphragm

c) Detail of diaphragm modeling

Figure 5: Overview of the numerical model of the bridge

The shell elements were used to model the concrete slab (Figure 6), the steel box, the vertical reinforcements near the arches' endings and the diaphragms and diagonals considered as critical for fatigue damage (Figure 7).

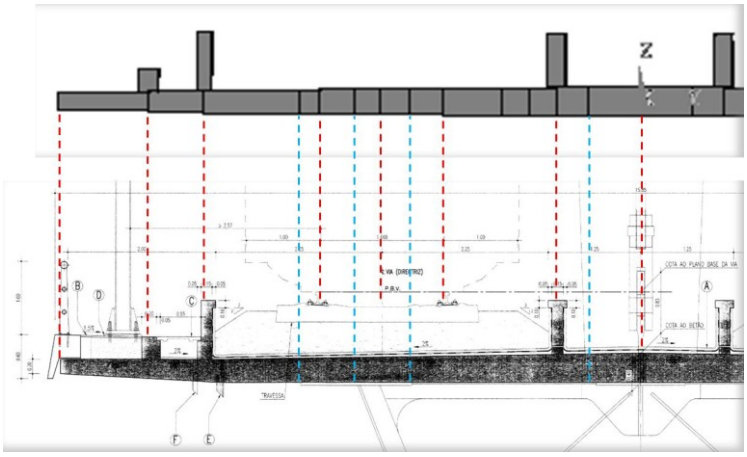

Figure 6: Alignments considered when modeling the concrete slab

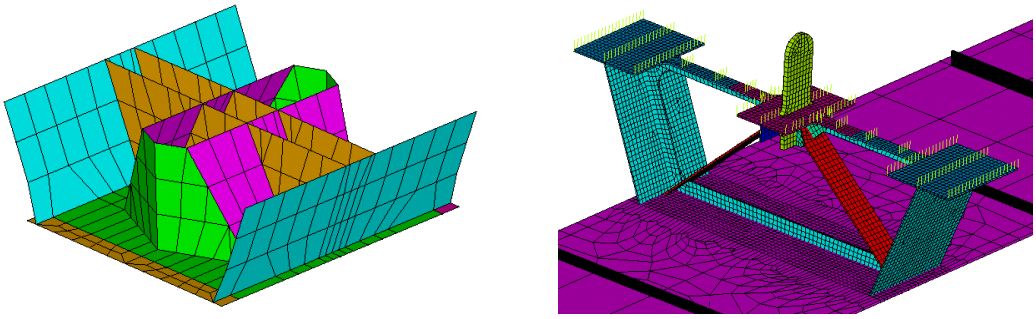

a) Vertical reinforcements at arches' endings

b) Critical diaphragm

Figure 7: Application of shell elements in the deck

The beam elements are used to model the arches, hangers, diaphragms and diagonals (Figure 8), stiffeners and ballast bearing beams.

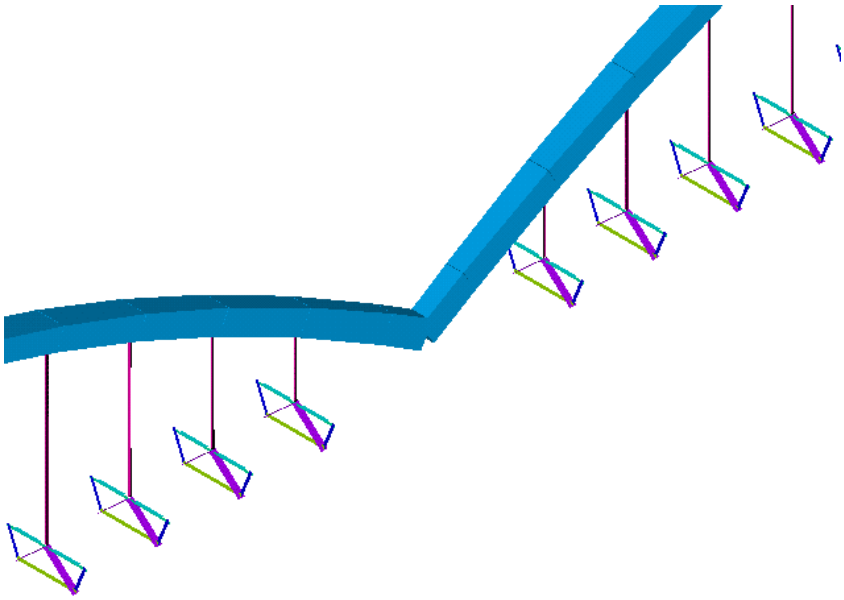

Figure 8: Beam elements: arches, hangers and diaphragms

Mass elements were used to reproduce the mass of the diaphragms of the arches. Rigid connections were also used between the concrete slab and the upper flanges of the steel box. After some sensitivity analysis, a 2m mesh dimension, in the longitudinal direction, was considered.

4 Experimental characterization of the structure

4.1 Ambient Vibration Test

4.1.1 Test procedure

Ambient Vibration Tests (AVT) are widely used around the world, to characterize the global dynamic characteristics of bridges. In the present case, a total of 33 deck sections and 19 arch sections were considered (Figure 9). Limitations on the total number of sensors available led to 20 different test setups. Compatibility between the different test setups was achieved by considering 8 reference points, distributed through 4 reference sections in the deck. Considered measurement points and directions at the sections of the deck and of the arches are shown in Figure 10.

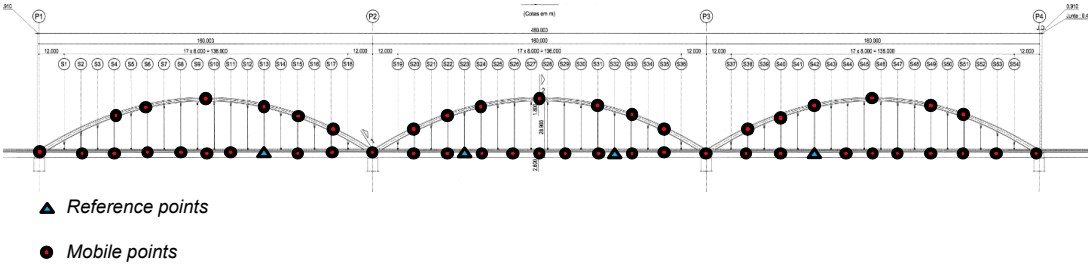

Figure 9: Measurement sections

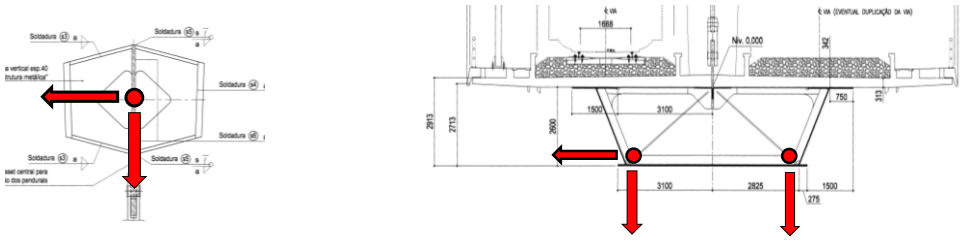

a) Sections of the arch b) Sections of the deck

Figure 10: Measurement points and directions

The acquisition equipment used was the National Instruments (NI) cDAQ-9172 with the NI 9233 IEPE analog input modules. The sensors consisted of 14 piezoelectric accelerometers (PCB model 393A03) with a sensitivity of about 1000 mV/g and a measuring range of ±5g. At each test setup a time series of 20 minutes was recorded at a sampling rate of 2000 Hz, decimated to 100 Hz. Due to the considerable length of the bridge, coaxial cables of up to 250 m were used to connect the sensors to the acquisition equipment, placed at the middle of the central span.

4.1.2 Test results

The data of the different time series obtained was processed with the software ARTEMIS. Two different algorithms were used, namely, the EFDD and the SSI-UPC Merged Test Setups algorithms. A relevant number of modes of vibration was found, namely vertical bending of the deck, torsion of the deck and transversal modes of the arches. The SSI-UPC algorithm, in particular, allowed distinguishing between close vibration modes, in narrow frequency bands. It also revealed to be a very efficient identification method, as it merges the records for all the test setups and only a single Stabilization Diagram is used [5]. Some of the referred vibration modes are compared with the numerical ones, in Figures 8 to 11.

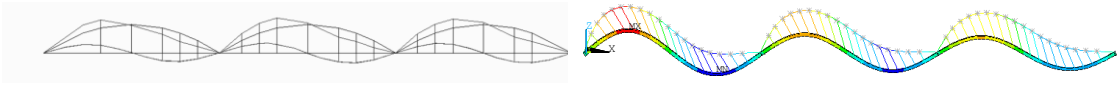

a) f_{exp} = 0.868 Hz b) f_{num} = 0.785 Hz

Figure 11: 1st vertical bending mode

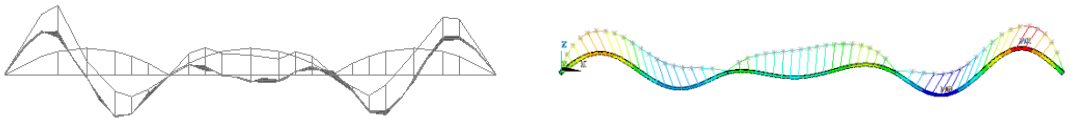

a) f_{exp} = 1.005 Hz b) f_{num} = 0.904 Hz

Figure 12: 2nd vertical bending mode

a) f_{exp} = 1.174 Hz b) f_{num} = 1.116 Hz

Figure 13: 3rd vertical bending mode

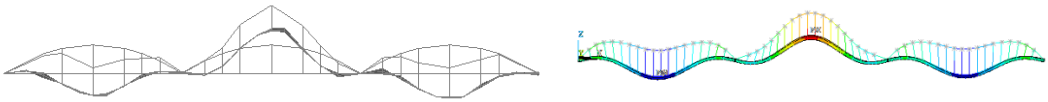

a) f_{exp} = 1.466 Hz b) f_{num} = 1.450 Hz

Figure 14: 4th vertical bending mode

In Table 1, the information on the frequency and damping ratios of the first eight vibration modes is summarized.

Mode number	Natural Frequency (Hz)			Damping (%)	Description
	Numerical	Experimental			
		SSI	EFDD		
1	0.785	0.868	0.868	1.630	Vertical bending mode
2	0.904	1.005	1.001	0.894	Vertical bending mode
3	1.116	1.174	1.180	0.522	Vertical bending mode
4	1.450	1.466	1.466	0.838	Vertical bending mode
5	2.052	2.075	2.074	1.296	Vertical bending mode
6	2.066	2.146	2.140	3.057	Torsion mode
7	2.190	2.179	2.190	2.728	Vertical bending mode
8	2.534	2.371	2.367	1.551	Vertical bending mode

Table 1: Frequencies and damping ratios of the experimental vibration modes

4.2 Long-term monitoring system

4.2.1 General description

The long-term monitoring system was developed in order to characterize the traffic and its corresponding effects at fatigue relevant points of the structure. Consequently, a traffic characterization system and a structural response characterization system are present. A trigger system controls the amount of recorded data. The acquisition system handles and stores the data, which is, after some local treatment sent to FEUP via a 3G wireless connection. The different systems are described below (Figure 15).

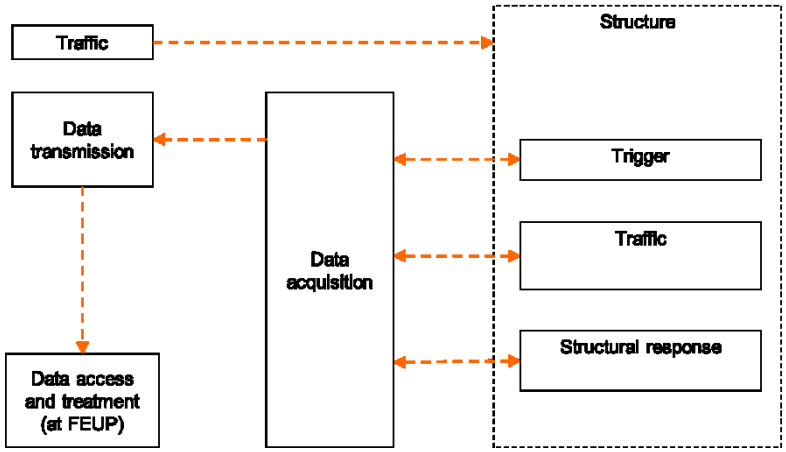

Figure 15: Long-term monitoring system

The traffic characterization system is performed both in qualitative and quantitative terms. Qualitative information is provided by an IP Camera placed at one hanger of the bridge (Figure 2 and Figure 16).

a) IP camera

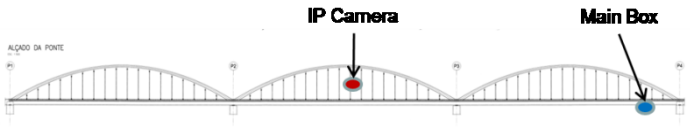

b) IP camera location

Figure 16: Qualitative traffic characterization

Quantitative information is provided by shear strain gages in the rails. These strain gages are placed at 3 different sections of the rail. At each section, a full Wheatstone bridge is installed. The difference between the shear strain at two consecutive measurement sections is proportional to the vertical load applied to the rail between them. This principle is the basis for the axle loads measurement [6].

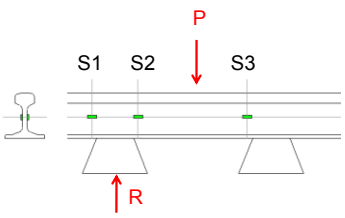

a) Location scheme

b) Installation

b) Protection

Figure 17: Strain gages in the rails

A total of 32 strain gages were bonded to the structure in reference points over 4 sections, as illustrated in Figure 18a). These locations were identified, with the aid of the developed FEM, as the more interesting in terms of fatigue damage analysis. Figure 18b) shows the locations of 11 strain gages placed at the section corresponding to Diaphragm 51.

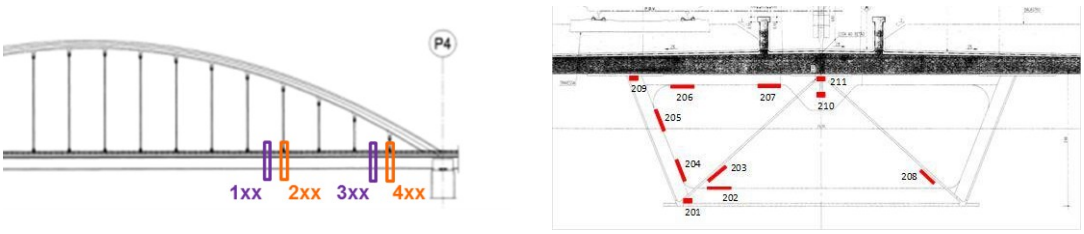

a) Sections b) Strain gages at Diaphragm 51

Figure 18: Strain gages location

Temperatures at the steel U-box girder are captured by 4 RTDs placed at the four corners of a single section, near Diaphragm 54.

The accelerations at the concrete slab and at the diagonals are recorded by 4 piezoelectric accelerometers with a sensitivity of 100 mV/g and a measurement range of ±50g.

Two vibration sensors are placed at a distance of 225 m from each extremity of the bridge and are used as triggers. Every time a high level of acceleration is reached, the data recording starts. As the triggers are far from the bridge, each load event (including the train approaching to the bridge) is fully recorded.

The data is acquired and processed by the National Instruments cRIO-9024 and, then, stored in a local disk and also sent, via a 3G connection, to a computer at FEUP.

4.2.2 Application - Commissioning phase

The long-term monitoring system was applied, during the commissioning phase, in the load test, planned by the Laboratório Nacional de Engenharia Civil (LNEC).

Three different types of vehicles were used to load the bridge: a single power engine machine (PEM), a short freight train (SFT) and a long freight train (LFT). In the case of the PEM, the axle loads where known with a high accuracy. Therefore, they were used on the calibration of the traffic characterization system.

In the case of the LFT, the different loading positions considered are illustrated in Figure 19.

For each position, the corresponding values of the strains were measured for all the strain gages. A very good agreement between the experimental and the numerical results was generally found.

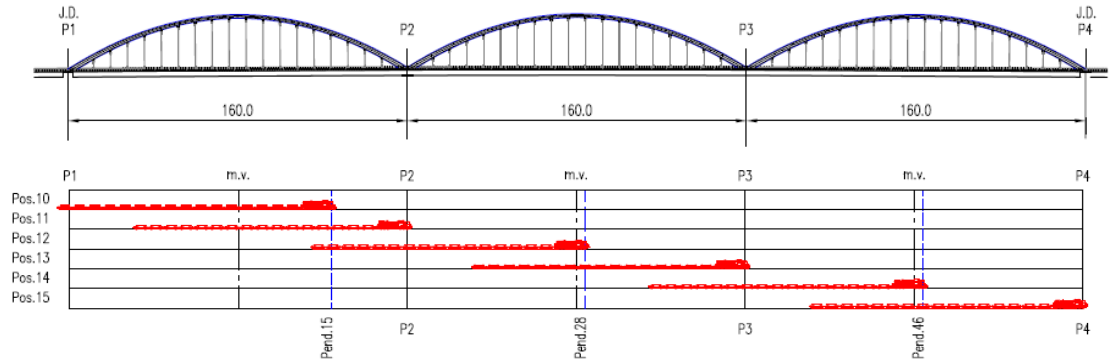

Figure 19: LFT positioning (adapted from [7])

Figure 20 displays a comparison between the experimental and numerical results, for the strain gages SG201 and SG203 (see Figure 18). SG201 measures longitudinal deformation on the bottom flange near diaphragm 51, while SG203 measures the deformation on one of the diagonals of the same diaphragm, in its axial direction.

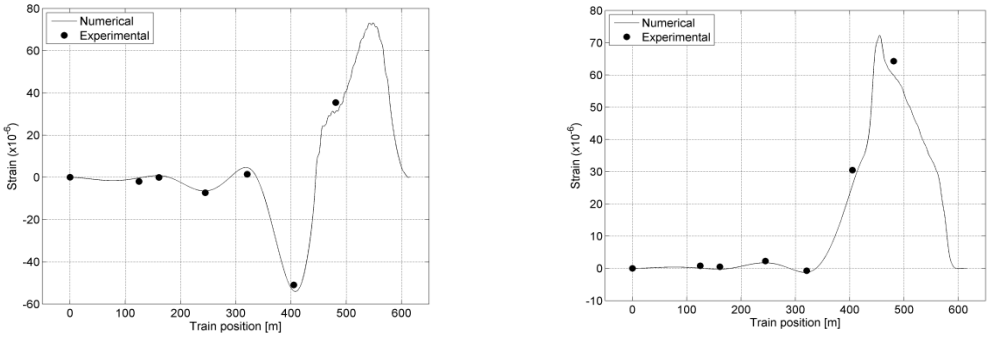

a) SG201 b) SG203

Figure 20: Experimental vs. Numerical strains due to LFT loading

Also in the context of this load test, the response of the bridge was obtained for a quasi static loading by the PEM running at a constant speed of 7 km/h. Once again, a very good agreement between the numerical estimate and the experimental results could be found. An example of the results obtained is provided in Figure 21.

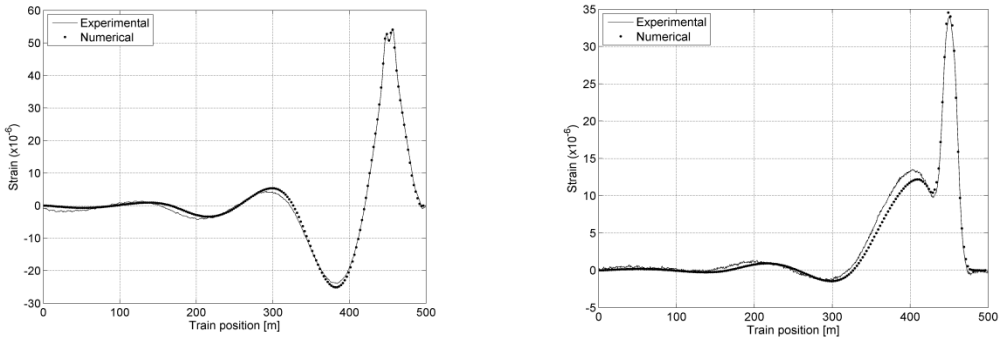

a) SG201 b) SG203

Figure 21: Experimental vs. Numerical strains due to quasi-static PEM loading

4.2.2 Application - Service phase

The traffic and the corresponding bridge's behaviour were monitored for a real traffic scenario. At this railway line, traffic is composed mainly by fast passenger trains, such as Alfa Pendular, with speeds up to 220 km/h, and heavy freight trains, proceeding from or to the sea port of Sines.

As the traffic loads are estimated, a good agreement can be found between experimental and numerical results. Figure 22 shows such type of comparison, for the case of Alfa Pendular tilting train passage.

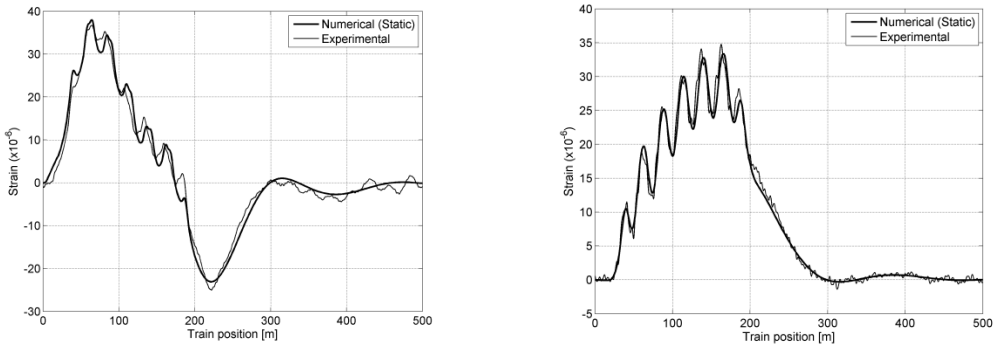

a) SG201 b) SG203

Figure 22: Experimental vs. Numerical strains due to Alfa Pendular loading

5 Fatigue and dynamic analysis

5.1 Identification and classification of fatigue prone details

The first step of the fatigue analysis was the identification and classification of bridge's fatigue prone details. This classification was based on the design information and also on visits to the bridge, during its construction phase. The most relevant details are:

- The extremities of the diagonals of the bridge (Figure 23);
- The welded elements transverse to the deck, such as diaphragms and stiffeners (Figure 24a));
- The connections between transverse beam and top side flanges, at each diaphragm.

Among all these details, the top connection of the diagonals of the last diaphragm of the bridge (Figure 25) revealed to be the most critical one.

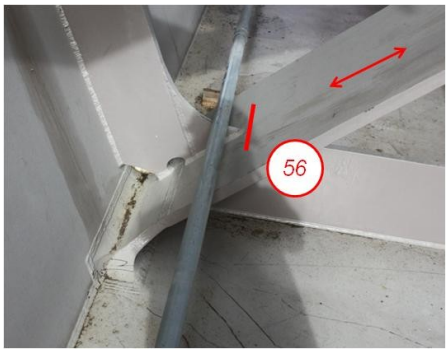

a) Top of the diagonal b) Bottom of the diagonal

Figure 23: Extremities of the diagonals

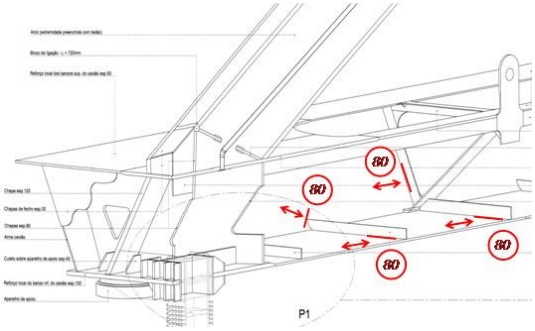

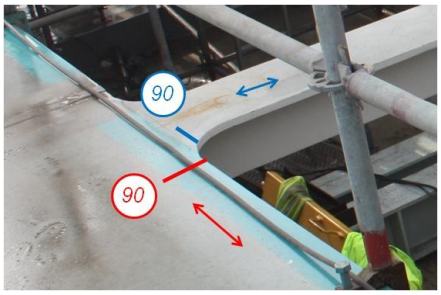

a) Welded elements transverse to the deck b) Transverse beam

Figure 24: Elements perpendicular to the longitudinal direction of the deck

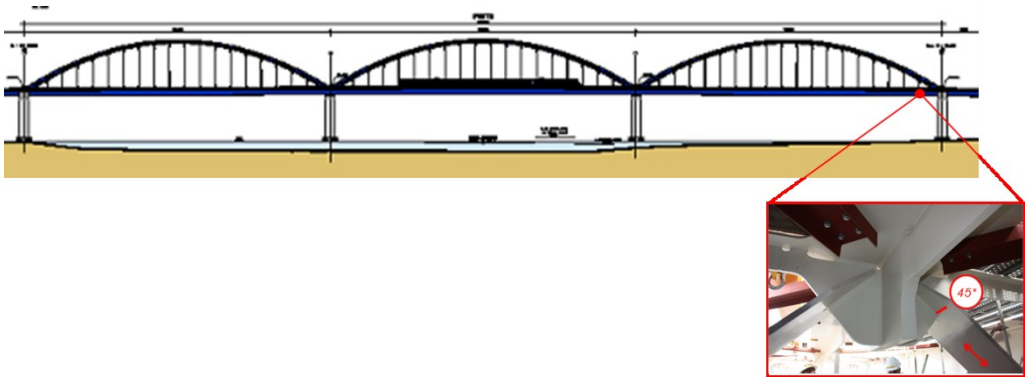

Figure 25: Critical detail

5.2 Fatigue damage

The different details were analysed according to the damage linear accumulation method, described in the Eurocode 3. Figure 26 illustrates the different stress history responses of the critical detail of the bridge to the passage of the 12 standard fatigue trains. In this case the most conditioning train was the FT 5.

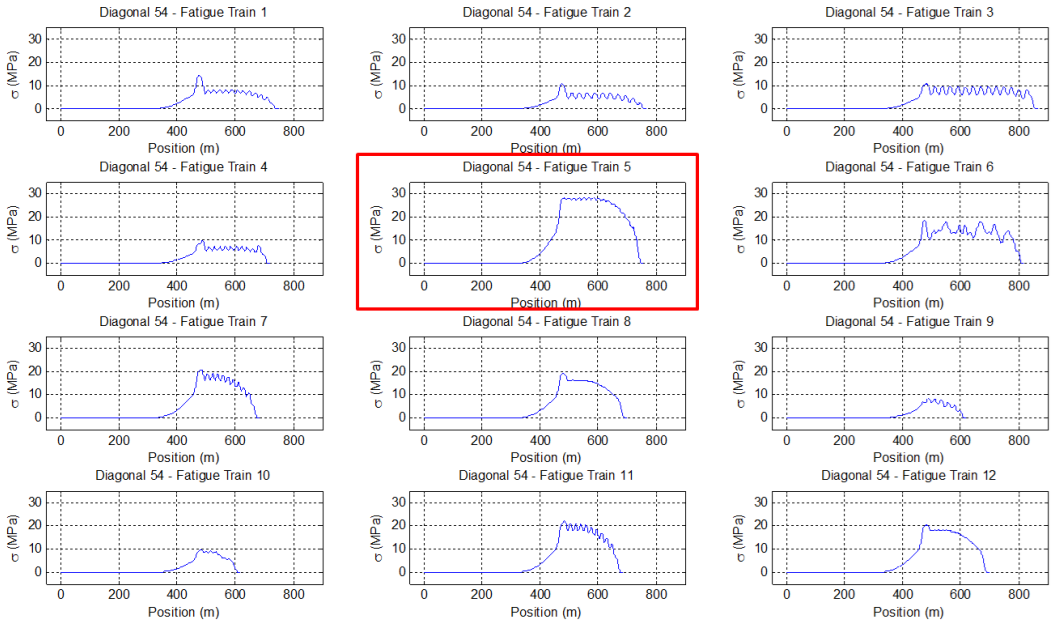

Figure 26: Stress histories in the critical detail, due to standard fatigue trains

Since the structure can held 2 tracks, the simultaneous crossing of trains over the bridge was also attended. A uniform probability distribution of the crossing points was considered.

In Figure 27 and Figure 28, the stress histories, at the critical detail, due to the simultaneous passage of two Standard Fatigue Trains, are presented. The difference between the two cases is the point where both trains cross each other.

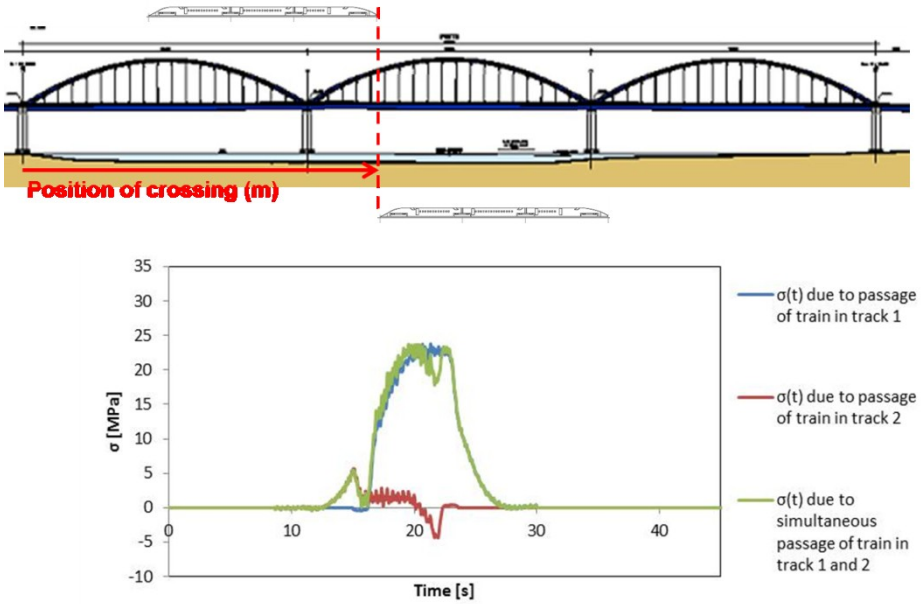

Figure 27: Stress history in the critical detail: crossing in the central span

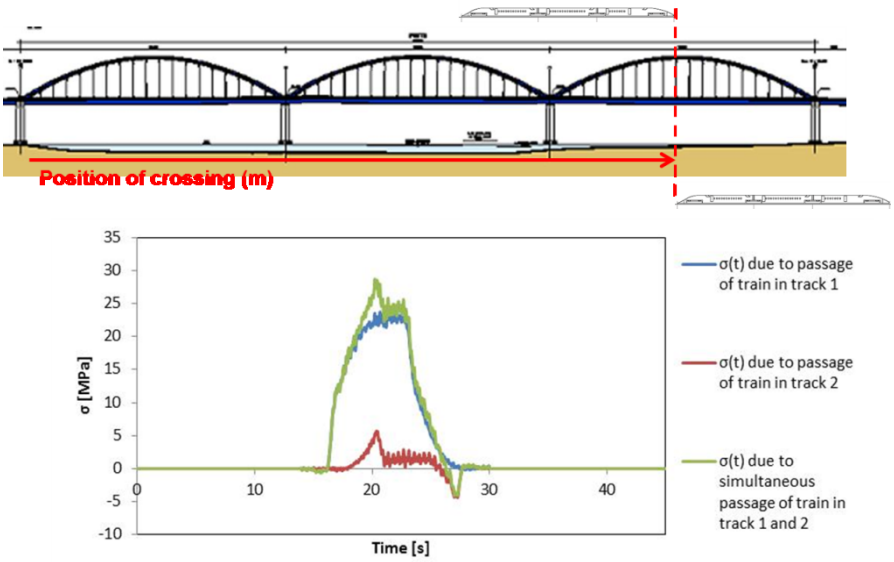

Figure 28: Stress history in the critical detail: crossing in the last span

Since different crossing points lead to different stress histories, the damage will also vary. That can be recognized by the different stress range histograms shown in Figure 29. In those histograms, the red line is the adequate Design Fatigue Strength Curve, according to Eurocode 3. The dashed line highlights the design value of the constant amplitude fatigue limit, $\Delta\sigma_D$. A summary of the fatigue damage obtained at the critical detail as a function of the crossing point of the two Standard Fatigue Trains is presented in Figure 30.

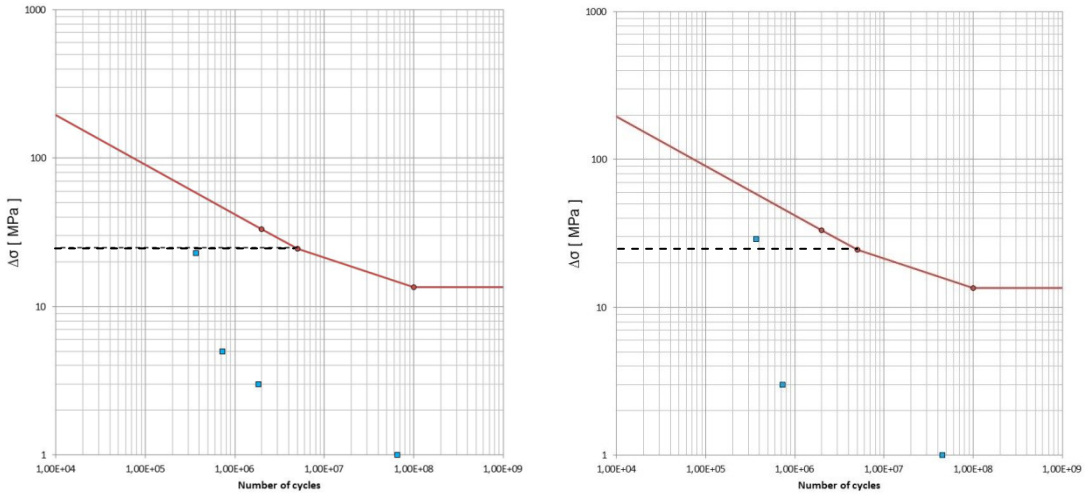

a) Crossing at central span b) Crossing at last span

Figure 29: Stress range histograms for different crossing points

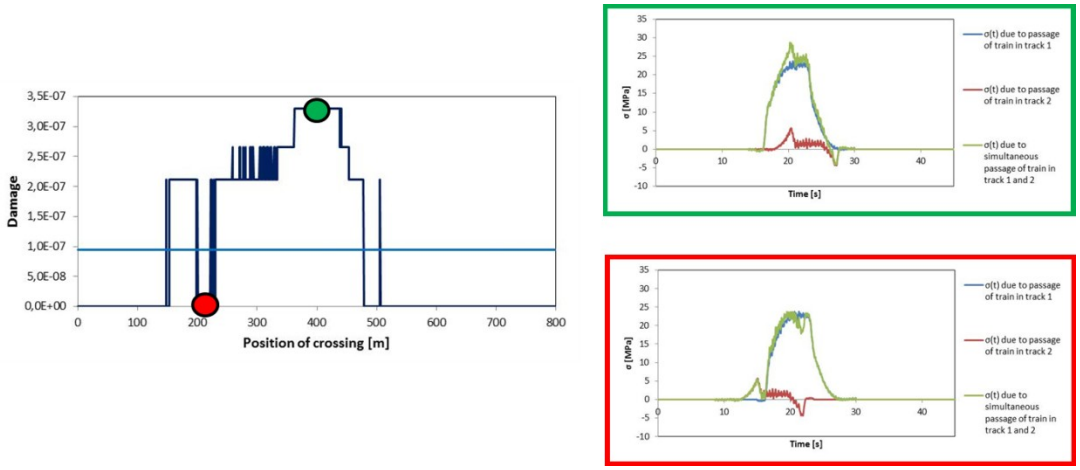

Figure 30: Damage in the critical detail as a function of the crossing point

Assuming that the crossing point has an uniform probability distribution, an average value of the damage for simultaneous crossings can be computed, D_{cross}. Total damage, D, including 12% of crossing events occurrence can then be computed by the following equation:

$$D = (100\%\text{-}12\%)\, D_{no\ cross} + 12\%\, D_{cross} \quad (1)$$

Equation (1) was used to compute the total damage at the critical detail, for the different traffic scenarios present in Eurocode 3. Each traffic scenario is defined in terms of variety and number of standard fatigue trains per day. In all cases, the annual damage obtained is very low (Figure 31).

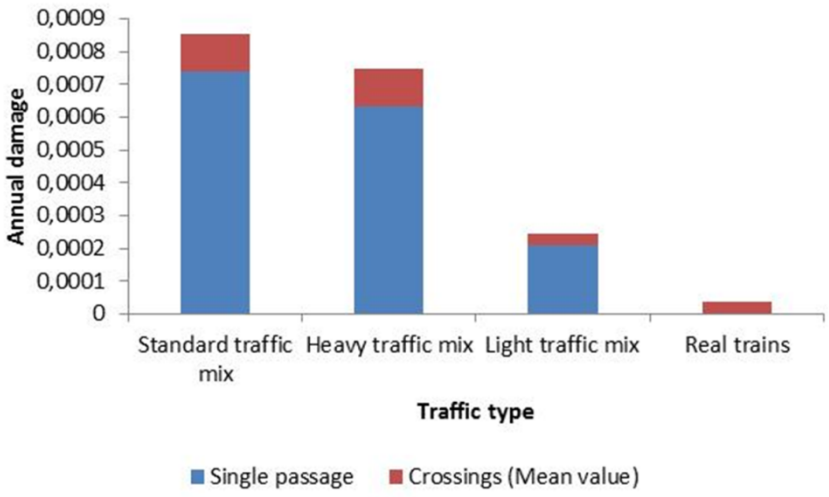

Figure 31: Damage in the critical detail for different traffic scenarios

5.3 Impact of local modes in total dynamic response

The different modes of vibration of the bridge have different impacts on its total dynamic response. In order to assess the contribution of higher frequency modes, the total response (Standard Fatigue Train 5), at the critical detail, obtained with the modal superposition method was decomposed into its different components (Figure 32).

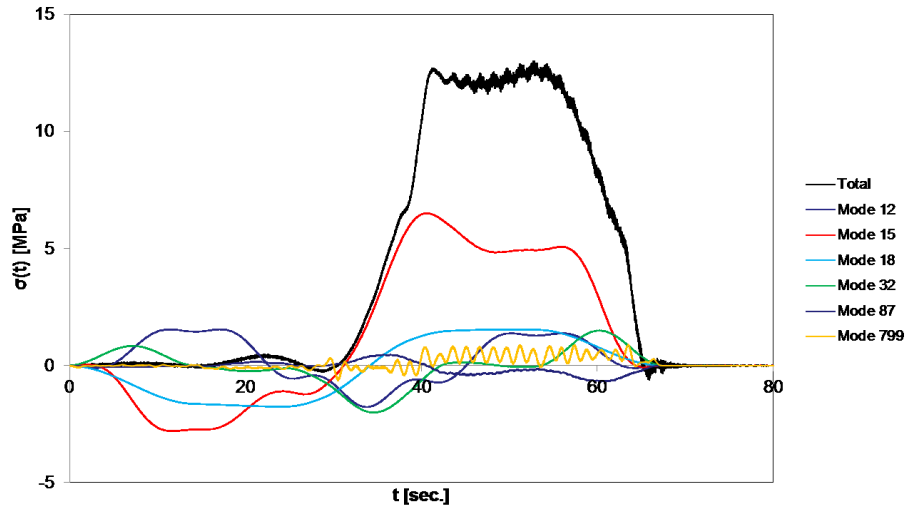

Figure 32: Contribution of different modes of vibration modes to the total response

The maximum stress range was then computed for an increasing number of modes, up to 30 Hz (Figure 33). It was observed that, in this case, the maximum stress range is controlled mainly by the global modes of vibration, with lower frequencies.

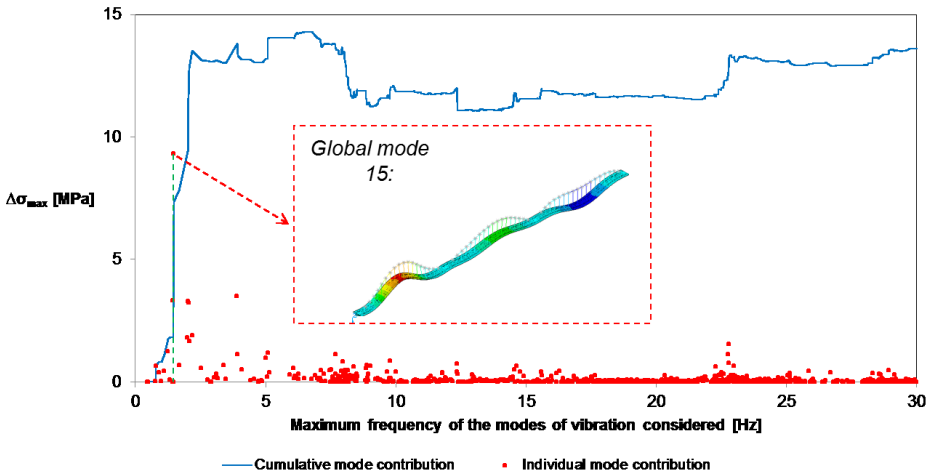

Figure 33: Contribution of different modes of vibration modes to the maximum stress range

6 Conclusions

The new Alcácer do Sal composite railway bridge is under study concerning its vibration induced and distortion induced fatigue behaviour. In this kind of analysis, the FEM of the structure is an important tool. Nevertheless, it is important to assure that the developed FEM reproduces well the response of the real structure.
In this context, an ambient vibration test of the bridge was performed and a large number of vibration modes were extracted, both with the EFDD and the SSI-UPC Merged Test Setups algorithms. The latter algorithm was especially efficient and allowed the extraction of different vibration modes contained in very narrow frequency bands. The results of the AVT will be used on the calibration of the developed FEM of the bridge.
A long-term monitoring system was also built to characterize the traffic and its corresponding effects at some fatigue relevant points of the structure. The system was applied both in a static load test and in operation.
The traffic characterization system was of paramount importance, as it allowed the comparison between the experimental and numerical results, which were, generally, in close agreement.
The FEM of the bridge allowed for fatigue analyses in different points of the structure and for different traffic scenarios.
The most critical detail was the top extremity of the diagonals of the last diaphragm of the bridge. For that detail, the worst loading case was the crossing of two Standard Fatigue Trains at the last span of the bridge. Even so, low damage levels are foreseen.
The global modes of vibration, with lower frequencies, are the most determinant to the total response of the bridge, at the critical detail.

Acknowledgements

The present work has been funded by the Portuguese Foundation for Science and Technology (FCT), in the context of the Research Project Advanced methodologies for the assessment of the dynamic behaviour of high speed railway bridges (FCOMP-01-0124-FEDER-007195), and by the European Commission, in the context of the Research Project FADLESS - Fatigue damage control and assessment for railway bridges (RFSR-CT-2009-00027). FCT scholarship SFRH/BD/47545/2008 is acknowledged. The authors also wish to acknowledge the collaboration and information provided by REFER and by LNEC.

References

[1] Eurocode 3: Design of steel structures. Part 1-9: Fatigue, EN 1993–1–9. European Committee for Standardisation, 2005.
[2] REFER, “Mapa da Rede”, 2011.

[3] REFER, "*The Alcácer Bypass"* (in Portuguese). Lisboa, 2010.
[4] GRID, "Alcácer Bypass: Design of the crossing of the river Sado" (in Portuguese), 2006.
[5] P. A. Döhler and L. Mevel, "Data Merging for Multi-Setup Operational Modal Analysis with Data-Driven SSI", in "Proc. 28th International Modal Analysis Conference (IMAC)", Jacksonville, USA, 2010.
[6] SUPERTRACK, "Final Report: Instrumentation, monitoring and physical modelling of high-speed lines", 2005.
[7] LNEC, "Static load test of the new railway crossing of the river Sado at the Alcácer Bypass" (in Portuguese), 2011